Kinetics and Mechanism of the Addition of Triphenylphosphonio-cyclopentadienide to Tetrahalo-*p*-benzoquinones. Part III.[1,2] The Disubstitution of Chloranil and Bromanil

Francisco Pérez Pla,[a] C. Dennis Hall,*[,b] Rosa Valero[a] and Manuel Pons[a]
[a] *Departamento de Química Física, Universidad de Valencia, Dr. Moliner 50, Burjassot 46100, Spain*
[b] *Department of Chemistry, King's College, London, UK WC2R 2LS*

Chloranil and bromanil react with an excess of triphenylphosphoniocyclopentadienide to yield the 2,5- and 2,6-disubstituted quinone derivatives through two parallel, second-order reactions. Kinetic data suggest that the reaction proceeds in two steps, involving addition to form a polar betaine intermediate followed by elimination of hydrogen halide. The activation parameters strongly suggest that the loss of halide is of the E_1 type. The empirical rate law has been established carrying out a multi-response non-linear least-squares analysis followed by a Gaussian de-convolution of the visible spectra of the reaction mixtures.

The reaction of triarylphosphoniocyclopentadienides **1** with tetrahalo-*p*-benzoquinones **2** proceeds to give monosubstituted products **3** in virtually quantitative yield which have been characterized by UV spectroscopy (λ = 700 nm), multi-nuclear NMR and X-ray crystallography.[3-5]

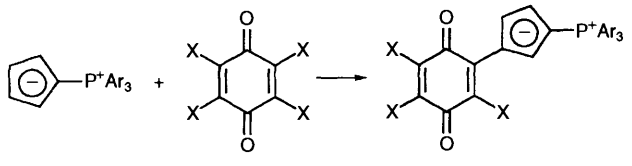

1 2 3

One of the important conclusions of this work was that the cyclopentadiene ring of **1** was substituted in position-3 in contrast with reactions with smaller electrophiles (*e.g.* aryl diazonium ions) which gave substitution in position-2 of the cyclopentadiene ring.[6,7] The kinetics and mechanism of this reaction have also been studied intensively for X = Cl[1] and X = Br, and I[2] and to some extent with X = F, with the conclusion that the reaction proceeds by the rate-limiting addition of the ylide to the quinone, followed by elimination of hydrogen halide by either an E_1, E_2, or E_1cB mechanism dependent upon the halide. It was suggested in fact, that with X = Cl, the mechanism of halide elimination was probably E_1cB whereas with X = I, the mechanism was probably E_1. With X = Br, the data were explained by either an E_2 or E_1cB mechanism with emphasis on the former. It was noted during these studies that the brilliant blue compounds formed by monosubstitution of the quinone, reacted further in the presence of an excess of ylide to form mixtures of compounds which were all intensely coloured. It is well known that the haloquinones undergo disubstitution (in the 2,5- or 2,6-position)[8-10] and that under forcing conditions, multiple substitution may occur.

This paper deals with the question of product identity from the disubstitution reactions and the kinetics and mechanism of disubstitution reaction with chloranil and bromanil.

Experimental

Materials.—Triphenylphosphoniocyclopentadienide was prepared by the method reported by Ramirez.[11] For kinetic runs further purification was carried out by flash chromatography on silica gel 60H using dichloromethane as the eluent. The quality of the purified product (>99%) was checked by IR and ^1H and ^{31}P NMR spectroscopy.

*Tetrahalo-*p*-benzoquinones.* The commercial products were recrystallized twice from acetone and then sublimed to give bright-yellow crystals. The quality of products was checked by IR spectroscopy.

Dichloromethane. The solvent was dried by distillation from calcium hydride. Only freshly distilled dichloromethane was used for kinetic runs.

Kinetic Experiments.—Stock solutions of chloranil (2.3×10^{-3} mol dm^{-3}) and bromanil (2.6×10^{-3} mol dm^{-3}) in CH_2Cl_2 were prepared and then diluted by a factor of ten. Six reaction mixtures were prepared by injecting 500μl of the quinone solution into a UV–VIS cell containing a fresh, thermostatted solution of ylide, prepared *in situ* by introducing into the cells a weighed quantity of ylide ranging from 2.5 mg to 30.0 mg and 2.5 cm^3 of CH_2Cl_2. The weight of the reaction mixture was checked at the end of the experiment in order to test for possible losses of solvent during the measurements.

The absorbance spectrum of the six reaction mixtures were recorded between 400 and 800 nm at intervals of 10 min during 1010 min for the choranil system and at intervals of 7 min during 707 min for the bromanil system with a Cary-3 UV–VIS spectrophotometer equipped with an automatic sample handler and controlled by a computer. The temperature was maintained constant to ±0.1 °C with the Peltier heater–cooler accessory of the machine. In each case 101 spectra were collected per kinetic experiment.

The procedure was repeated at 273.2, 283.2, 293.2, 303.2 and 311.2 K for chloranil and at 288.2, 293.2, 303.2 and 311.2 K for bromanil. At low temperatures a nitrogen flow was maintained inside the sample compartment to avoid water condensation. An additional experiment was carried out at 293.2 K for choranil but using a solution 10^{-4} mol dm^{-3} of quinuclidine as the base in CH_2Cl_2 as the solvent.

Synthetic Procedure.—A solution containing (80 mg, 0.24 mmol) of ylide **1** in dichloromethane (10 cm^3) was prepared at room temp. and then added to a solution containing (30 mg, 0.12 mmol) of chloranil in dichloromethane (50 cm^3) cooled to 5 °C. A solution (300 mg, 3.0 mmol) of triethylamine in dichloromethane (5 cm^3) was added and the mixture was allowed to react for 72 h at 5 °C. Addition of *n*-hexane (50 cm^3) precipitated the product which was filtered off and redissolved in dichloromethane.

Isomer Separation.—The crude reaction product was dissolved in CH_2Cl_2 (3 cm^3) and deposited on a TLC plate

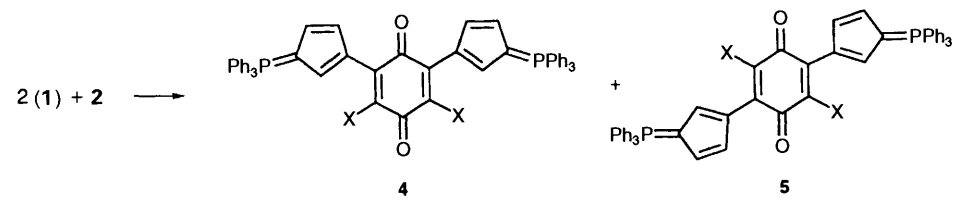

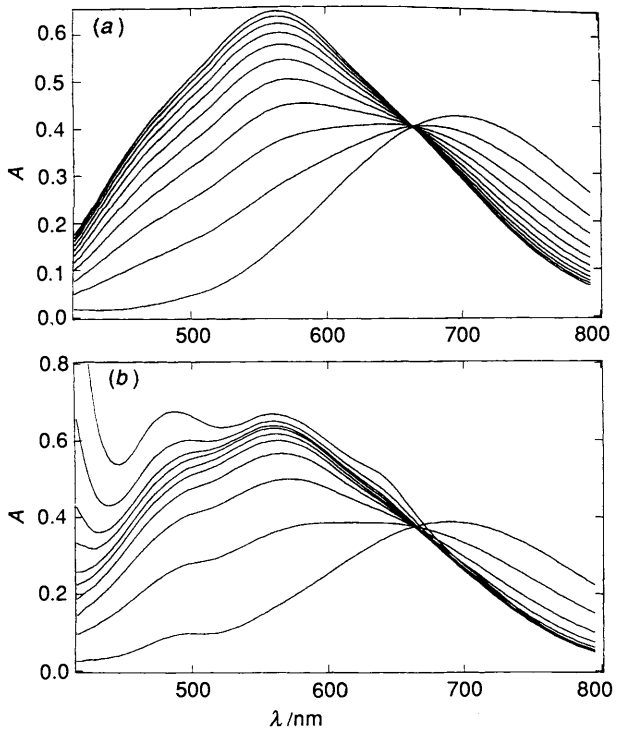

Fig. 1 Visible spectra of reaction mixtures: (*a*) reaction mixture at 283.2 K containing 4.3 × 10^{-5} mol dm^{-3} chloranil and 1.59 × 10^{-3} mol dm^{-3} ylide; (*b*) reaction mixture at 311.2 K containing 4.0 × 10^{-5} mol dm^{-3} chloranil and 1.7 × 10^{-3} mol dm^{-3} ylide

(20 × 20 cm) prepared by mixing silica gel (20 g) and water (40 cm^3) and dried in an oven at 70 °C overnight. A mixture of dichloromethane (10%) and diethyl ether (90% v/v) was used as the eluent. Under these conditions two bands were observed. The first violet band contained the 2,5-disubstituted isomer **5** and the second broad, green band contained the 2,6-disubstituted isomer **4**. Both fractions were extracted from the silica with a mixture of dichloromethane (90%) and diethyl ether (10% v/v). Further purification was achieved by repeating the chromatography three times. The 2,5-isomer (violet band) was found to be unstable and decomposed to a large extent during the separation procedure.

The pure isomers were obtained as lustrous dark-green and violet powders after precipitation with *n*-hexane and drying under vacuum. The compounds were characterized by multinuclear NMR spectroscopy and mass spectrometry (see Tables 1 and 2).* The violet isomer was unstable in solution, decomposing especially at higher concentration, and its characterization by NMR spectroscopy was therefore poor relative to that of the green compound.

* It should be noted that in view of the unambiguous ^{13}C assignments of the carbonyl groups in **4** and **5**, the assignments of the C=O groups in the monosubstituted products **3** (ref. 2) are incorrect. The C=O group at *ca.* δ 180 in **3** should be assigned to C(4) and the C=O group at *ca.* δ 172 should be assigned to C(1).

Results and Discussion

Structure Determination.—The mass spectrometry data and in particular the IR spectra, leave no doubt, that the purple compound is the 2,5-isomer and the green compound is the 2,6-isomer. For both X = Cl and X = Br the IR spectra of the green compounds show two carbonyl stretching vibrations (at 1655 and 1614 cm^{-1} for X = Cl and at 1658 and 1617 cm^{-1} for X = Br) as required for the 2,6-isomer. With the symmetrical 2,5-isomer, however, only one carbonyl stretch is observed (at 1637 cm^{-1} for X = Cl and at 1635 cm^{-1} for X = Br). Substitution in the 2,3-positions, although possible, is much less likely in view of the expected level of steric hindrance in such a molecule. The origin of the instability of the 2,5-isomer remains a mystery but the rate of decomposition increases with the concentration of the solution which strongly suggests an intermolecular rather than an intramolecular process.

Kinetic Data.—After mixing, the monosubstituted product was formed in a matter of seconds in a quantitative yield, so its concentration was considered identical with that of the parent haloquinone.

The spectrum of the ylide interferes in the 400–450 nm region so the spectra of reaction mixtures were corrected by subtracting the ylide spectrum multiplied by an appropriate dilution factor. This correction did not affect the kinetic results since the ylide was in a large excess and therefore its concentration may be considered as constant. Typical spectra recorded from reaction mixtures at 283.2 and 311.2 K are shown in Fig. 1 at various time intervals. The shape of each set of spectra depends on the temperature at which the reaction is carried out and on the concentration of ylide. At low temperature, the spectrum shows only a decreasing absorbance from the monosubstituted compound (at 690 nm) and the appearance of a new broad band around 550–560 nm due to the disubstituted products. An isosbestic point (λ = 663 nm for chloranil and λ = 661 nm for bromanil) exists between these two bands indicating that the new species are formed at the expense of the monosubstituted product with no detectable intermediate. At high temperature, the spectra show the appearance of a new band centred at 405 nm and a general distortion of the spectrum towards the end of the observation time. By this time, the isosbestic point has been lost indicating the existence of a parallel reaction which does not involve the quinone ring.

The band at 405 nm, which increases in proportion to the ylide concentration, is due to a parallel reaction that involves the ylide and its protonated species **6–8**. When a dichloromethane solution of ylide is treated with an excess of CF_3CO_2H the cyclopentadiene ring is protonated mostly in position C(3), as demonstrated by the $^1H,^1H$ COSY NMR spectrum, see Fig. 2. The data show quite clearly that the protonation of ylide **1** see Scheme 1, may be represented by the equilibrium of **6**, **7** and **8**, in which most of the cyclopentadiene proton signals arise from **6** with a weak–weak interaction (H^2 at 7.48 ppm) a strong–weak interaction (H^4 at 7.26 ppm) and another strong–weak interaction (H^5 at 6.87 ppm).

The visible and ^1H NMR spectra of the protonated ylide remain unchanged over several days but when a solution of ylide is treated at 314 K with a small (less than one equivalent)

Table 1 Spectroscopic data on the 2,6-disubstituted products

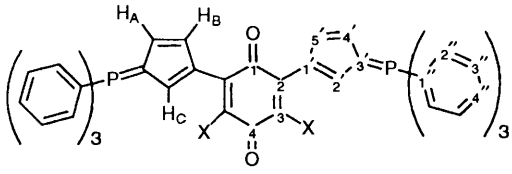

^{13}C NMR spectrum

	X = Cl			X = Br	
Assignment	δ	J_{P-C}/Hz	DEPT	δ	J_{P-C}/Hz
C(1)	173.50 (s)	0.0	0	174.01 (s)	0.0
C(2)	142.74 (d)	2.1	0	146.89 (d)	2.0
C(3)	122.32 (s)	0.0	0	115.40 (s)	0.0
C(4)	190.50 (s)	0.0	0	191.05 (s)	0.0
C(1′)	121.12 (d)	19.4	0	122.89 (d)	19.2
C(2′)	126.57 (d)	16.3	+	127.33 (d)	16.3
C(3′)	87.34 (d)	111.0	0	87.99 (d)	110.9
C(4′)	120.11 (d)	14.9	+	121.01 (d)	14.8
C(5′)	117.17 (d)	14.1	+	117.70 (d)	16.3
C(1″)	123.89 (d)	90.4	0	124.66 (d)	90.4
C(2″)	133.30 (d)	10.3	+	134.11 (d)	10.3
C(3″)	128.82 (d)	12.5	+	129.62 (d)	12.4
C(4″)	132.86 (d)	2.8	+	133.66 (d)	2.9

^{1}H NMR spectrum

Assignment	δ	J/Hz		
X = Cl				
H(Ph)	7.62 (multiplet, 30 H)			
H(A)	6.86 (octet, 2 H)	J_{AB} = 4.4	J_{AC} = 2.1	J_{AP} = 5.5
H(B)	6.27 (octet, 2 H)		J_{BC} = 2.1	J_{BP} = 3.0
H(C)	7.05 (sextet, 2 H)			J_{CP} = 5.5
X = Br				
H(Ph)	7.63 (multiplet, 30 H)			
H(A)	6.85 (octet, 2 H)	J_{AB} = 4.4	J_{AC} = 2.2	J_{AP} = 5.6
H(B)	6.28 (sextet, 2 H)		J_{BC} = 2.1	J_{BP} = —
H(C)	7.13 (sextet, 2 H)			J_{CP} = 5.7

^{31}P NMR spectrum

X = Cl: δ 14.53 (s) X = Br: δ 14.55 (s)

FAB mass spectrum

X = Cl:[a] M = 824 (11.2), M + 1 (86.2), M + 2 (71.0), M + 3 (100), M + 4 (61.2), M + 5 (50.9), M + 6 (27.3)
X = Br:[b] M = 912 (0.92), M + 1 (32.5), M + 2 (100), M + 3 (54.1)

ν(KBr disk)/cm^{-1}

X = Cl
3055w (H stretch Ph), 2953w, 2923w, and 2853w (H stretch cp), 1665m and 1614m (C=O stretch), 1566m, 1518s, 1483w, 1458s, 1437s, 1334m, 1295m, 1244m, 1194m, 1139s, 1114s, 1093vs, 1032s, 999w, 974w, 944w, 931w, 840w, 809w, 782m, 753m, 721s, 696s, 645s, 613w, 565s, 531m and 517m

X = Br
3055w (H stretch Ph), 2955w, 2925w, 2858w (H stretch cp), 1658w and 1617m (C=O stretch), 1560m, 1514s, 1457s, 1438s, 1337m, 1294w, 1185m, 1136s, 1109s, 1087s, 1049w, 997w, 968w, 943w, 919w, 807w, 753w, 720s, 693s, 626s, 571s, 530m and 511m

λ_{max}(CH_2Cl_2)/nm at 298 K (400–800 nm)

X = Cl		X = Br	
λ_{max}/nm	ε_{max}/dm^3 mol^{-1} cm^{-1}	λ_{max}/nm	ε_{max}/dm^3 mol^{-1} cm^{-1}
464	9 540	467	10 050
643	10 340	635	11 050

[a] In thioglycerol matrix. [b] In *m*-nitrobenzyl alcohol matrix.

Table 2 Spectroscopic data on the 2,5-disubstituted compound

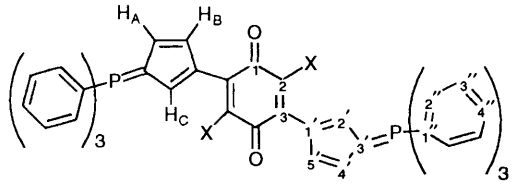

^{13}C NMR spectrum

	X = Cl			X = Br	
Assignment	δ	J_P/Hz	DEPT	δ	J_P/Hz
C(1)	180.5 (s)	0.0	O		
C(2)	128.5 (s)	0.0	O		
C(3)	140.5 (s)	—	O		
C(1′)	121.5 (d)	—	O		
C(2′)	128.7 (d)	—	+		
C(3′)	91.4 (d)	127	O		
C(4′)	118 (d)	—	+		
C(5′)	116 (—)	—	+		
C(1″)	125 (d)	90.5	O		
C(2″)	134.18 (d)	10.3	+	134.00 (d)	10
C(3″)	129.68 (d)	12.4	+	129.23 (d)	12
C(4″)	133.68 (d)	2.7	+	133.46 (d)	3

^{1}H NMR spectrum

Assignment	δ	J/Hz		
X = Cl				
H(A)	7.02 (octet)	J_{AB} = 4.4	J_{AC} = 2.1	J_{AP} = 5.6
H(B)	6.26 (octet)		J_{BC} = 2.2	J_{BP} = 3.0
H(C)	7.04 (sextet)			J_{CP} = 5.5
X = Br				
H(A)	6.85 (octet)	J_{AB} = 4.4	J_{AC} = 2.2	J_{AP} = 5.6
H(B)	6.24 (multiplet)		J_{BC} = 2.1	J_{BP} = —
H(C)	7.13 (sextet)			J_{CP} = 5.7

^{31}P NMR spectrum

X = Cl: δ/ppm = 14.57 (s) X = Br: δ/ppm = 14.56 (s)

FAB mass spectrum

X = Cl:[a] M = 824 (7.1), M + 2 (46.5), M + 3 (100), M + 4 (50.6), M + 5 (66.7), M + 6 (57.8), M + 7 (30.5)
X = Br:[b] M = 912 (50.1), M + 2 (25.4), M + 3 (100), M + 4 (59.4), M + 5 (44.8), M + 6 (26.7), M + 7 (7.9)

ν(KBr disk)/cm^{-1}

X = Cl
3055w (H stretch Ph), 2954w, 2922w, and 2853w (H stretch cp), 1637m (C=O stretch), 1516m, 1457s, 1437s, 1333m, 1291w, 1205w, 1120vs, 1050w, 1032s, 942w, 840w, 868w, 805w, 720m, 696s, 673m, 612w, 568m, 532m and 513m

X = Br
3055w (H stretch Ph), 2952w, 2924w, and 2851w (H stretch cp), 1635m (C=O stretch), 1514m, 1457s, 1435s, 1331m, 1290w, 1189w, 1109vs, 1038w, 940w, 852w, 805w, 753w, 719m, 693s, 647m, 627m, 605m, 564m, 532m and 512m

$\lambda_{max}(CH_2Cl_2)$/nm at 298 K (400–800 nm)

	λ_{max}/nm	ε_{max}/dm^3 mol^{-1} cm^{-1}
X = Cl	553	27 300
X = Br	557	21 800

[a] In thioglycerol matrix. [b] In *m*-nitrobenzyl alcohol.

quantity of acid, the visible, ^{1}H and ^{31}P NMR spectra change in a matter of hours. The visible spectrum shows an intense band at 405 nm and four weak bands at (481, 553, 637 and 720 nm) and the ^{31}P NMR spectrum shows a broad band at 13.77 ppm whereas the ylide has a sharp band at 13.68 ppm. This reaction was followed during two days and by the end of the second day the ^{31}P NMR spectrum showed at least 12 signals (11.69, 13.75, 14.80, 15.16, 15.53, 15.62, 15.91, 16.07, 16.52, 16.80, 17.63 and 18.17 ppm) the Ph_3P peak −4.97 ppm and the Ph_3P=O peak 28.02 ppm. Clearly, a complicated oligomerization reaction occurs which involves elimination of Ph_3P and either oxidation or adventitious hydrolysis to Ph_3P=O.

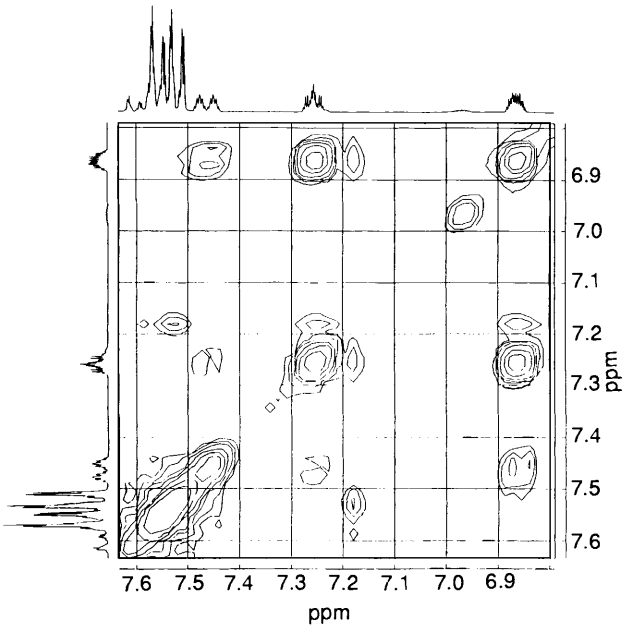

Fig. 2 $^1H,^1H$ COSY NMR spectrum (360 MHz) of a mixture containing 21 mg of ylide (0.064 mmol) and 41 mg of trifluoroacetic acid (0.36 mmol) in 1.31 g of deuteriated dichloromethane (15 mmol) at room temperature

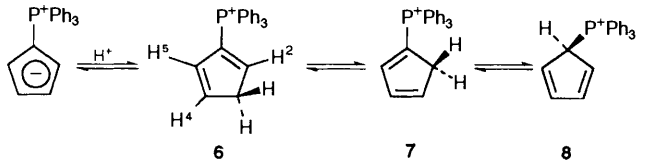

Scheme 1

Interpretation of the Kinetic Data.—A first attempt to analyse the absorbance data was carried out assuming a first-order decrease in concentration of monosubstituted compound, a logical hypothesis since the ylide was in a large excess. For this purpose, five wavelengths were selected (λ = 413, 550, 460, 640 and 690 nm—the observed absorption maxima for mono- and di-substituted products) and absorbance values at each wavelength were plotted *vs.* time. The curves behaved exponentially at low temperature as indicated by the Guggenheim plots. Under these conditions, the plots consisted of five parallel straight lines but at 311.2 K, especially in the 400 nm region, the Guggenheim plots were curved. It was noticed that the plots became more curved as the concentration of ylide increased. These results can be explained by a first-order model complicated by the existence of a slow parallel reaction involving the ylide. Fig. 3 shows typical Guggenheim plots at 283.2 and 311.2 K.

Several empirical equations were tested by a 'trial and error' procedure to take into account the variation of absorbance *vs.* time as accurately as possible. The best results were obtained when empirical eqn. (1) was used, where $A_\lambda(t)$ is the absorbance

$$A_\lambda(t) = \beta_{0\lambda} + \beta_{1\lambda}e^{-kt} + \beta_{2\lambda}e^{\mu t}, (k, \beta_{2\lambda} \text{ and } \mu > 0) \quad (1)$$

at wavelength 'λ' and time 't', $\beta_{i\lambda}$ are constants at a fixed wavelength and k and μ are positive constants. The calculation of the adjustable parameter set $\{\beta_i,k,\mu\}$ was performed by minimizing the least-squares multi-response surface [see eqn. (2)], related to eqn. (1) by means of the Davidon–Fletcher–Powell method using a modified version of the OPKINE[12,13]

$$\chi^2 = \sum_\lambda \sum_i [A_{\lambda i} - (\beta_{0\lambda} + \beta_{1\lambda}e^{-kt_i} + \beta_{2\lambda}e^{\mu t_i})]^2 \quad (2)$$

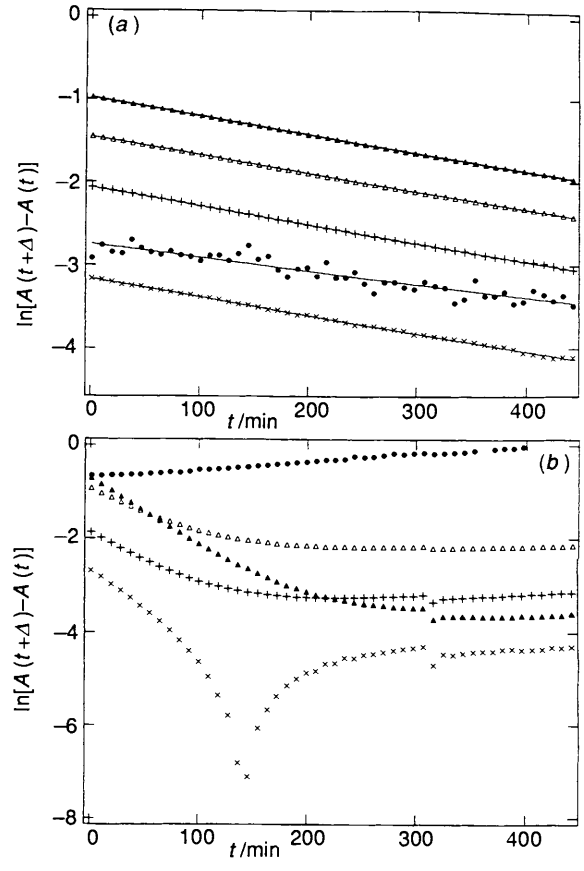

Fig. 3 Guggenheim absorbance *vs.* time data plots: (*a*) reaction mixture at 273.2 K containing 4.6 × 10^{-5} mol dm^{-3} chloranil and 2.17 × 10^{-3} mol dm^{-3} ylide; (*b*) reaction mixture at 311.2 K containing 4.0 × 10^{-5} mol dm^{-3} chloranil and 1.7 × 10^{-3} mol dm^{-3} ylide; ●, 413; △, 460; ▲, 550; +, 640 and ×, 690 nm

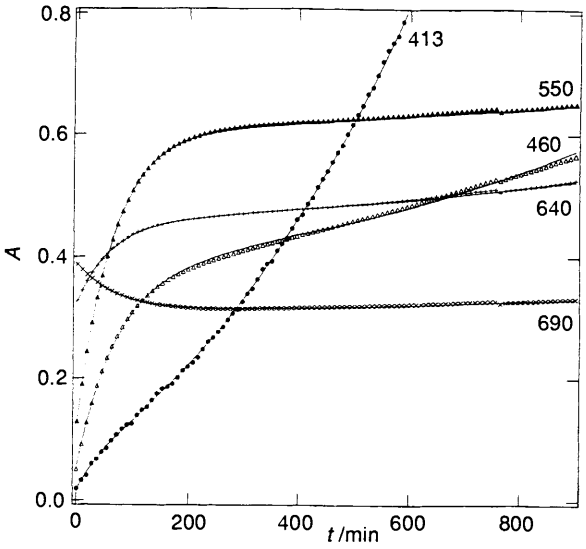

Fig. 4 Absorbance *vs.* time plot of a reaction mixture containing 4.3 × 10^{-5} chloranil and 1.59 × 10^{-3} mol dm^{-3} ylide at 311.2 K. The solid lines are the non-linear fits to the experimental data; ●, 413; △, 460; ▲, 550, +, 640 and ×, 690 nm.

program. In eqn. (2), the subscript 'λ' refers to a wavelength, and subscript 'i' refers to time. The calculated values of k parameters are shown in Table 3. The k values obtained from Guggenheim plots and the non-linear optimization method are essentially the same. It was found that the first and second terms of eqn. (1) explain the absorbance behaviour below 293.2 K, the

Table 3 First-order kinetic coefficients for the chloranil-ylide system

T/K	$y_o/10^{-3}$ mol dm^{-3}	$q_o/10^{-5}$ mol dm^{-3}	$k/10^{-3}$ min^{-1} [a]	$k/10^{-3}$ min^{-1} [b]	$1 + r$	$k_g/10^{-3}$ min^{-1}	$k_v/10^{-3}$ min^{-1}
273.2 ± 0.1	4.23	4.26	0.4 ± 0.4	0.41 ± 0.07	1.903 ± 0.009	0.21 ± 0.07	0.19 ± 0.07
	5.27	4.49	0.5 ± 0.1	0.55 ± 0.02	1.905 ± 0.006	0.29 ± 0.03	0.26 ± 0.03
	7.49	4.52	0.7 ± 0.4	0.72 ± 0.01	1.925 ± 0.007	0.37 ± 0.01	0.34 ± 0.01
	11.57	4.51	1.2 ± 0.1	1.17 ± 0.01	1.915 ± 0.005	0.61 ± 0.01	0.56 ± 0.01
	17.10	4.56	1.7 ± 0.1	1.75 ± 0.01	1.955 ± 0.007	0.90 ± 0.01	0.86 ± 0.01
	21.67	4.59	2.2 ± 0.2	2.24 ± 0.01	1.909 ± 0.007	1.17 ± 0.01	1.07 ± 0.01
283.2	5.07	4.17	0.5 ± 0.3	0.94 ± 0.03	1.867 ± 0.005	0.51 ± 0.03	0.44 ± 0.03
	8.36	4.20	0.9 ± 0.4	1.52 ± 0.06	1.871 ± 0.007	0.81 ± 0.08	0.71 ± 0.08
	10.06	4.23	1.2 ± 0.1	1.83 ± 0.09	1.873 ± 0.008	0.98 ± 0.12	0.85 ± 0.12
	13.84	4.23	1.8 ± 0.1	2.55 ± 0.01	1.873 ± 0.014	1.36 ± 0.02	1.19 ± 0.02
	15.90	4.31	2.5 ± 0.1	2.94 ± 0.01	1.886 ± 0.011	1.56 ± 0.02	1.38 ± 0.02
293.2	2.85	4.10	0.90 ± 0.05	0.94 ± 0.01	1.837 ± 0.004	0.51 ± 0.01	0.43 ± 0.01
	4.08	5.34	1.29 ± 0.07	1.37 ± 0.01	1.846 ± 0.006	0.74 ± 0.01	0.63 ± 0.01
	8.16	4.13	2.40 ± 0.13	2.47 ± 0.01	1.854 ± 0.007	1.33 ± 0.01	1.14 ± 0.01
	10.85	4.08	3.27 ± 0.13	3.35 ± 0.01	1.847 ± 0.014	1.82 ± 0.03	1.54 ± 0.03
	12.88	4.16	3.87 ± 0.15	4.08 ± 0.01	1.865 ± 0.007	2.18 ± 0.02	1.89 ± 0.02
	17.06	4.15	5.10 ± 0.20	5.34 ± 0.02	1.894 ± 0.014	2.82 ± 0.04	2.52 ± 0.04
293.2[c]	4.92	2.71	—	1.60 ± 0.01	1.87 ± 0.05	0.85 ± 0.01	0.74 ± 0.01
	10.06	2.81	—	3.30 ± 0.02	1.866 ± 0.02	1.77 ± 0.01	1.53 ± 0.01
	14.87	2.85	—	4.99 ± 0.01	1.884 ± 0.005	2.65 ± 0.02	2.34 ± 0.02
	20.14	2.86	—	7.18 ± 0.03	1.862 ± 0.006	3.86 ± 0.01	3.32 ± 0.01
	24.55	2.91	—	8.78 ± 0.03	1.869 ± 0.004	4.70 ± 0.03	4.08 ± 0.03
	29.55	2.91	—	10.72 ± 0.07	1.881 ± 0.005	5.70 ± 0.10	5.02 ± 0.10
303.2	2.82	4.07	1.4 ± 0.2	1.60 ± 0.01	1.733 ± 0.008	0.92 ± 0.01	0.68 ± 0.01
	4.86	4.18	2.5 ± 0.2	2.81 ± 0.01	1.736 ± 0.011	1.62 ± 0.02	1.19 ± 0.02
	8.17	4.17	4.2 ± 0.4	4.64 ± 0.01	1.759 ± 0.009	2.64 ± 0.03	2.00 ± 0.03
	10.31	4.17	5.4 ± 0.4	5.82 ± 0.03	1.763 ± 0.011	3.30 ± 0.05	2.52 ± 0.05
	12.87	4.17	6.7 ± 0.8	7.27 ± 0.04	1.772 ± 0.007	4.10 ± 0.05	3.17 ± 0.05
	15.75	4.16	8.4 ± 1.0	9.00 ± 0.05	1.780 ± 0.009	5.05 ± 0.07	3.94 ± 0.07
311.2	2.86	3.99	2.0 ± 0.5	2.41 ± 0.01	1.679 ± 0.010	1.43 ± 0.01	0.97 ± 0.01
	4.89	4.14	3.7 ± 0.4	4.45 ± 0.02	1.693 ± 0.011	2.63 ± 0.04	1.82 ± 0.04
	8.23	4.19	6.4 ± 0.9	7.27 ± 0.04	1.724 ± 0.006	4.22 ± 0.05	3.06 ± 0.05
	10.82	4.17	8.4 ± 1.7	9.66 ± 0.07	1.736 ± 0.011	5.54 ± 0.09	4.08 ± 0.09
	13.70	4.19	11.0 ± 1.5	12.15 ± 0.10	1.748 ± 0.011	6.95 ± 0.13	5.20 ± 0.13
	17.05	4.02	13.5 ± 2.4	14.45 ± 0.10	1.737 ± 0.013	8.32 ± 0.06	6.13 ± 0.06
First-order kinetic coefficients for the bromanil–ylide system[d]							
288.2 ± 0.1	5.82	6.83		2.68 ± 0.05	2.08 ± 0.01	1.29 ± 0.06	1.39 ± 0.06
	12.75	6.85		5.55 ± 0.05	2.07 ± 0.01	2.68 ± 0.06	2.87 ± 0.06
	16.87	6.90		7.21 ± 0.10	2.07 ± 0.01	3.48 ± 0.10	3.72 ± 0.10
	20.37	6.82		8.93 ± 0.10	2.05 ± 0.01	4.35 ± 0.10	4.58 ± 0.10
	25.13	6.77		11.24 ± 0.10	2.07 ± 0.01	5.43 ± 0.10	5.81 ± 0.10
	30.37	6.76		13.19 ± 0.10	2.06 ± 0.01	6.40 ± 0.10	6.79 ± 0.10
293.2 ± 0.1	5.49	3.16		3.81 ± 0.05	1.96 ± 0.01	1.95 ± 0.06	1.86 ± 0.06
	9.88	3.19		6.28 ± 0.05	2.08 ± 0.01	3.02 ± 0.06	3.26 ± 0.06
	14.56	3.22		9.21 ± 0.10	2.04 ± 0.01	4.51 ± 0.10	4.69 ± 0.10
	19.69	3.22		12.86 ± 0.10	2.09 ± 0.01	6.16 ± 0.10	6.70 ± 0.10
	24.19	3.23		15.28 ± 0.10	2.11 ± 0.01	7.24 ± 0.10	8.04 ± 0.10
	30.19	3.21		19.02 ± 0.10	2.14 ± 0.01	8.87 ± 0.10	10.14 ± 0.10
303.2 ± 0.1	4.85	3.09		5.88 ± 0.05	2.05 ± 0.01	2.87 ± 0.06	3.01 ± 0.06
	9.73	3.09		11.10 ± 0.05	2.05 ± 0.01	5.41 ± 0.06	5.69 ± 0.06
	14.42	2.92		16.44 ± 0.10	2.09 ± 0.01	7.85 ± 0.10	8.58 ± 0.10
	19.64	3.10		22.60 ± 0.10	2.10 ± 0.01	10.74 ± 0.10	11.85 ± 0.10
	24.81	3.09		28.74 ± 0.10	2.09 ± 0.01	13.74 ± 0.10	15.00 ± 0.10
	29.76	3.08		34.51 ± 0.10	2.10 ± 0.01	16.41 ± 0.10	18.09 ± 0.10
311.2 ± 0.1	4.44	6.49		7.71 ± 0.05	2.01 ± 0.01	3.77 ± 0.06	3.95 ± 0.06
	8.04	6.50		12.69 ± 0.10	2.05 ± 0.01	6.31 ± 0.06	6.30 ± 0.06
	16.02	6.46		25.55 ± 0.10	2.00 ± 0.01	12.77 ± 0.10	12.78 ± 0.10
	19.88	6.48		31.75 ± 0.10	2.03 ± 0.01	15.64 ± 0.10	16.11 ± 0.10
	24.92	6.52		40.97 ± 0.10	2.02 ± 0.01	20.27 ± 0.10	20.69 ± 0.10
	28.90	6.57		47.65 ± 0.10	2.03 ± 0.01	23.50 ± 0.10	24.16 ± 0.10

[a] Coefficients obtained using Guggenheim's method. [b] Coefficients obtained by non-linear multi-response minimization. [c] Coefficients obtained from solutions 1.0×10^{-4} mol dm^{-3} in quinuclidine. [d] q_o: Initial concentration of tetrahalo-*p*-benzoquinone; y_o: initial concentration of triphenylphosphoniocyclopentadienide; k_g: first-order rate coefficient governing the appearance of the 2,6-isomer; k_v: first-order rate coefficient governing the appearance of the 2,5-isomer.

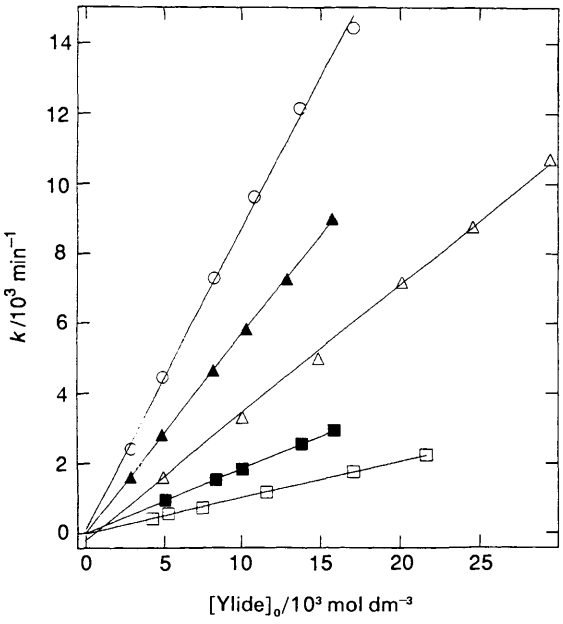

Fig. 5 Dependence of the first-order kinetic coefficient, k, on the initial concentration of ylide and temperature: □, 273.2; ■, 283.2; △, 293.2; ▲, 303.2 and ○, 311.2 K

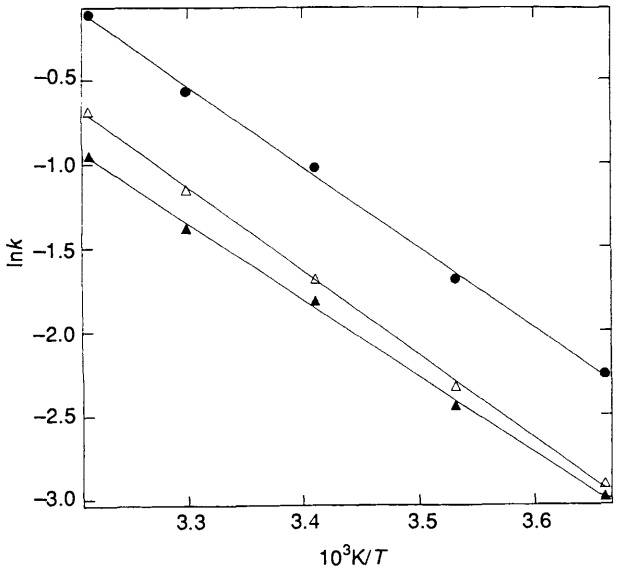

Fig. 6 Arrhenius plots of the second-order △, $k_g^{(2)}$; ▲, $k_v^{(2)}$ and ●, $k^{(2)}$ kinetic coefficients

second exponential only becoming important above 303.2 K. In Fig. 4, the solid lines represent the fits to the sets of data points.

Plots of k *vs.* the initial ylide concentration (y_o) gave good straight lines (Fig. 5), at all temperatures. The fact that the intercepts of the lines were zero allows the conclusion that the monosubstituted product **3** does not decompose spontaneously during the time of observation. The Arrhenius plot applied to the slopes of these lines also gave a good straight line (Fig. 6). These facts indicate that k behaves as a kinetic coefficient governing the disappearance of the monosubstituted compound.

The same treatment was applied to the μ values but a definite variation of μ with y_o was observed only above 303.2 K for chloranil. A linear relationship was also found between μ and y_o at 311.2 K [$\mu = (4.6 \pm 0.6) \times 10^{-4} + (0.084 \pm 0.05)\, y_o$].

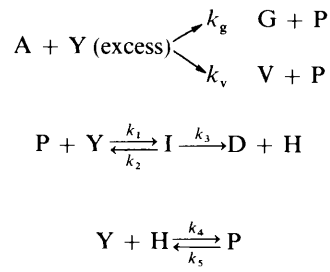

A = monosubstituted product **3**, G = 2,6-disubstituted product **4**, V = 2,5-disubstituted product **5**, P = protonated species of ylide, Y = ylide, I = intermediate, H = form of the free proton in the solvent, D = product responsible for the absorbance at 405 nm at high temperature. The concentration of each species is represented by lowercase letters.

Scheme 2

Once the empirical rate law was established, the next step was to provide a mechanistic interpretation of the kinetic data. Several mechanisms were tested, but the mechanism in Scheme 2 gave the best explanation of the rate data. From the mechanism it is clear that:

$$-\dot{a} = (k_g + k_v)a = ka, \qquad a = a_o e^{-kt} \tag{3}$$

$$\dot{g} = k_g a, \qquad g = a_o \frac{k_g}{k}(1 - e^{-kt}) \tag{4}$$

$$\dot{v} = k_v a, \qquad v = a_0 \frac{k_v}{k}(1 - e^{-kt}) \tag{5}$$

Assuming that the ylide and its protonated species are in equilibrium with an intermediate species, I, which decomposes to the product D (λ = 405 nm) we can write:

$$K_1 = \frac{i}{yp}, \qquad i = K_1 yp \approx K_1 y_0 p \tag{6}$$

Applying the stationary steady hypothesis we obtain the following expression for the concentration of H:

$$\dot{h} = k_3 i - k_4 yh + k_5 p \approx 0, \qquad h \approx \left(\frac{k_3}{k_4} K_1 + \frac{k_5 1}{k_4 y_o}\right) p \tag{7}$$

With the aid of eqn. (7) it is possible to integrate p. First, the differential rate equation for P is written:

$$\dot{p} = ka - k_1 yp + k_2 i + k_4 yh - k_5 p \tag{8}$$

The substitution of h from eqn. (7) in (8) leads to eqn. (9) whose solution is given by eqn. (10).

$$\dot{p} - \mu p = a_o k e^{-kt}, \qquad \mu = \frac{k_1 k_3}{k_2} y_o \tag{9}$$

$$p = a_o \frac{k}{k + \mu}(e^{\mu t} - e^{-kt}) \tag{10}$$

Assuming that decomposition of I is rate limiting, we can then write:

$$\dot{d} = k_3 i \approx k_3 K_1 y_o p = a_o \frac{k\mu}{k + \mu}(e^{\mu t} - e^{-kt}) \tag{11}$$

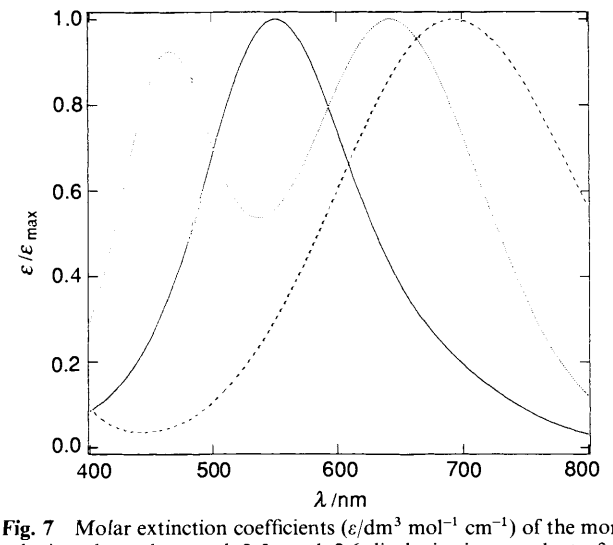

Fig. 7 Molar extinction coefficients (ε/dm^3 mol^{-1} cm^{-1}) of the monosubstituted product and 2,5- and 2,6-disubstitution products from chloranil at 298.2 K. (——) 2,5-isomer, ε_{max} = 27 300; (• • • •) 2,6-isomer, ε_{max} = 10 340; (– – –) monosubstituted, ε_{max} = 9800 dm^3 mol^{-1} cm^{-1}.

$$d = a_o \frac{k\mu}{k + \mu}\left(\frac{1}{-\mu}e^{\mu t} + \frac{1}{k}e^{-kt} - \frac{k + \mu}{k\mu}\right) \quad (12)$$

Thus it is possible to write the following equation for the absorbance at each wavelength:

$$A(t) = \varepsilon_a a(t) + \varepsilon_g g(t) + \varepsilon_v v(t) + \varepsilon_d d(t) + \varepsilon_p p(t) \quad (13)$$

where it is assumed the species H does not absorb in the visible. Substituting the values of a, g, v, d and p in eqn. (13) we obtain eqn. (14).

$$\frac{A}{a_o} = \left\{\frac{\varepsilon_g k_g + \varepsilon_v k_v}{k} - \varepsilon_d\right\} + \left\{\varepsilon_a - \frac{\varepsilon_g k_g + \varepsilon_v k_v}{k} + \frac{\varepsilon_d \mu - \varepsilon_p k}{k + \mu}\right\}e^{-kt} + \frac{k}{k + \mu}(\varepsilon_d + \varepsilon_p)e^{\mu t} \quad (14)$$

The absorbance represented by eqn. (14) has the same form as that of eqn. (1) and is consistent with the experimental facts since it explains the absorbance *vs.* time data. Furthermore, if μ is small, for example at low temperatures or at low concentrations of ylide, the last term is virtually a constant and the Guggenheim equation is followed. This is the case below 303.2 K. The last term is also small when ε_d is small, for example at $\lambda > 550$ nm and in this region the Guggenheim equation will also be closely obeyed, as observed. Finally, the dependence of μ on the initial concentration of ylide is linear and β_3 and μ are greater than zero as observed.

Resolution of k *into* k_g *and* k_v.—The k coefficient was resolved into its k_g and k_v components, the rate coefficients which govern the appearance of disubstituted isomers, by using the following procedure. Dividing eqn. (3) by eqn. (4) and integrating leads to eqn. (15).

$$-\frac{da}{dg} = \frac{k}{k_g} = 1 + \frac{k_v}{k_g} = 1 + r, \qquad a = a_o - (1 + r)g \quad (15)$$

Eqn. (15) is the basis of our treatment. If the concentration of the monosubstituted compound is plotted against the concentration of one of the disubstituted products a straight line is obtained the slope of which gives information about the ratio of the kinetic coefficients, r, which govern the formation of both isomers. The species **3** and **4** were chosen for this treatment because they were the most stable.

From eqn. (15) it follows that it is necessary to know the molar extinction coefficients of **3** and **4** as accurately as possible in order to calculate the concentration of isomers at any time. In practice, however, it is not possible to use this information alone, since the spectra are perturbed by the parallel reaction suffered by the ylide. To avoid this problem a Gaussian analysis of the spectra of the reaction mixtures has been performed based on the visible spectra of compounds **3**, **4** and **5**.

Modelling of Visible Spectra.—The spectra of solutions of compounds **3**, **4** and **5** in dichloromethane were recorded between 400 and 800 nm at several concentrations and temperatures. The molar extinction coefficients at selected wavelengths and at each temperature were calculated from the molar concentration of each compound taking into account the density of the solvent at each temperature. The resultant molar extinction coefficients are shown in Fig. 7 as a function of wavelength at 298.2 K.

The next step was to formulate an empirical mathematical model which gave the value of ε as a function of wavelength and temperature. For this purpose, each curve $\varepsilon(\lambda)$ was fitted by non-linear least squares to a Gaussian series [eqn. (16)], where α_i, β_i and λ_i are adjustable parameters. The

$$\varepsilon(\lambda;T) = \sum_{i=1}^{n} \alpha_i(T)e^{-\frac{1}{2}\left(\frac{\lambda - \lambda_i}{\beta_i(T)}\right)^2} \quad (16)$$

value of λ_i was maintained constant for all temperatures. After fitting, the dependence of each parameter, α_i and β_i, on temperature was analysed. The majority of α_i values vary linearly with temperature whilst β_i coefficients behave as quadratic functions.

Gaussian Analysis of Reaction Spectra.—The Gaussian analysis of spectra was performed in the following way. At each temperature, the spectra from the solution having the greater concentration of ylide was selected. This solution was the most appropriate to carry out the first fitting as its spectrum showed the greater absorbance and the calculations performed on it were the most sensible. This spectrum was fitted by the least-squares procedure to eqn. (17):

$$\chi^2 = \sum_{\lambda}[A(\lambda) - \hat{A}(\lambda)]^2 \quad (17)$$

where:

$$\hat{A}(\lambda) = \sum_{i=1}^{2} \alpha_i e^{-\frac{1}{2}\left(\frac{\lambda - \lambda_i}{\beta_i}\right)^2} + \varepsilon_a(\lambda)a + \varepsilon_g(\lambda)g + \varepsilon_v(\lambda)v \quad (18)$$

Eqn. (18) consists of two sets of terms. The Gaussian set takes into account the variation of absorbance due to the parallel reaction of ylide. The second set takes into account the variation of absorbance the origin of which is the substitution reaction under investigation. The ε_i coefficients are functions of wavelength and temperature which had been calculated previously.

The set of variables to be evaluated by the minimization of χ^2 is now (α_i, λ_i, σ_i, a, g and v) and, in consequence, χ^2 is not a linear function of such variables. However, once λ_i and β_i were calculated from a spectrum, they were regarded as constant parameters in the remaining calculations at the same temperature. This is justified since, provided Beer's law is obeyed, λ_i and σ_i must remain constant among spectra differing only in the relative amount of absorbing species. The advantage of the procedure is that eqn. (17) becomes linear when λ_i and σ_i are considered as fixed parameters which saves a considerable amount of calculation time.

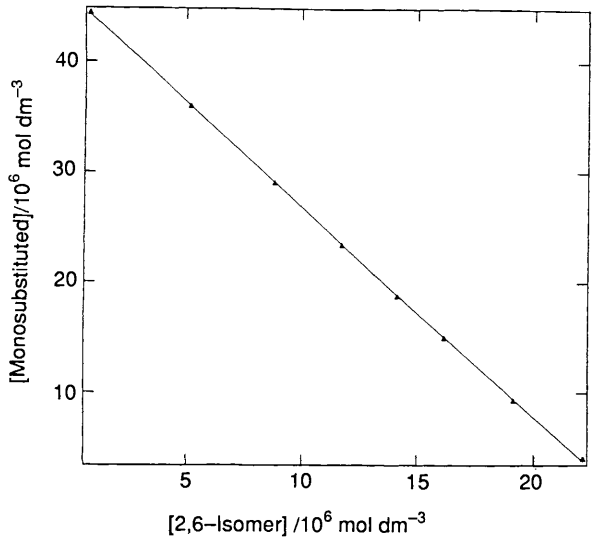

Fig. 8 Plot of the concentration of the monosubstituted product *vs.* the concentration of the 2,6-isomer of a reaction mixture containing 4.3×10^{-5} chloranil and 1.59×10^{-3} mol dm^{-3} ylide at 283.2 K

Table 4 Second-order kinetic coefficients for the chloranil–ylide and the bromanil–ylide systems as a function of temperature

	$k_i = h_i + k_i^{(2)}[y]_o$, h_i/min$^{-1} \approx 0$, $k_i^{(2)}$/mol dm^{-3} min^{-1}		
T/K	$k^{(2)}$	$k_g^{(2)}$	$k_v^{(2)}$
Chloranil–ylide system			
273.2 ± 0.1	0.105 ± 0.002	0.054 ± 0.001	0.050 ± 0.001
283.2	0.185 ± 0.002	—	0.087 ± 0.001
293.2	0.373 ± 0.006	0.198 ± 0.003	0.174 ± 0.004
293.2[a]	0.360 ± 0.007	0.194 ± 0.005	0.166 ± 0.002
303.2	0.567 ± 0.005	0.316 ± 0.002	0.251 ± 0.002
311.2	0.892 ± 0.011	0.504 ± 0.008	0.388 ± 0.003
Bromanil–ylide system			
288.2	0.436 ± 0.008	0.212 ± 0.004	0.224 ± 0.005
293.2	0.622 ± 0.009	0.285 ± 0.006	0.337 ± 0.005
303.2	1.15 ± 0.01	0.546 ± 0.005	0.609 ± 0.006
311.2	1.64 ± 0.03	0.810 ± 0.012	0.813 ± 0.017

[a] In the presence of quinuclidine 1.0×10^{-4} mol dm^{-3}.

Eight spectra equally separated in absorbance and covering one order of magnitude in the concentration of the monosubstituted and disubstituted products were then selected from each reaction mixture. The spectra were deconvolved by minimizing eqn. (17) and the variable a was plotted against variable g for each fitting. In all cases good straight lines were obtained, see Fig. 8, the slope being then $(1 + r)$. The values of the slopes are collected in Table 3 and, in order to test the validity of results, ln(a) was plotted *vs.* time. Good straight-lines were obtained in all cases, their slopes being essentially the same as those obtained by the Guggenheim method or those obtained by fitting eqn. (1).

The values of k_g and k_v were calculated from k and r. They are shown in Table 4, and as expected, they vary linearly with the initial concentration of ylide (Fig. 9). The Arrhenius plot of the slopes are also good straight lines. We may conclude that k_g and k_v are the kinetic coefficients of formation of the disubstituted compounds.

Interpretation of k_g *and* k_v.—In previous work,[1,2] we demonstrated that the rate-limiting step for the formation of monosubstituted products between the ylide and tetrahalo-*p*-

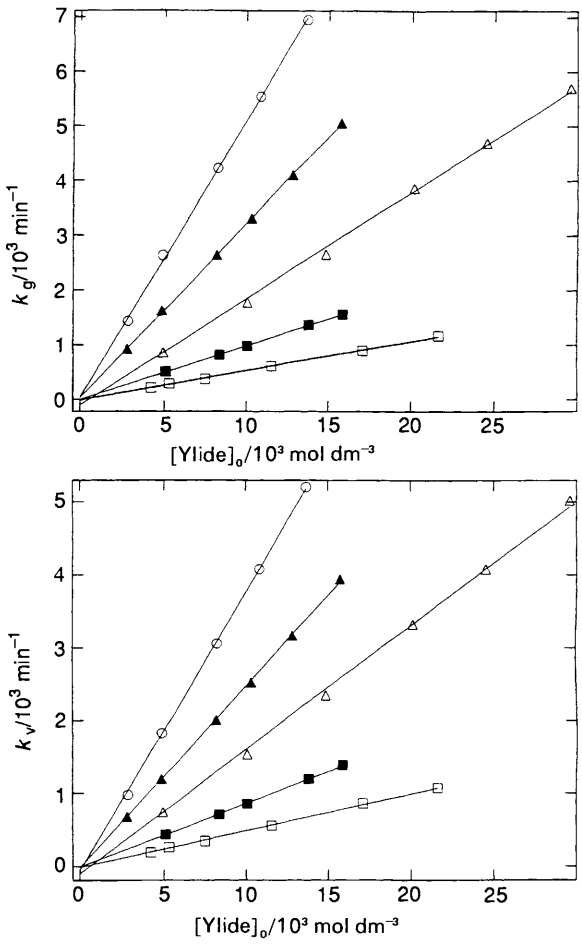

Fig. 9 Dependence of first-order kinetic coefficients k_g and k_v on the initial concentration of ylide and temperature: □, 273.2; ■, 283.2; △, 293.2; ▲, 303.2 and ○, 311.2 K

benzoquinones was the nucleophilic attack by the cyclopentadiene ring of the ylide on the electron deficient quinone. The elimination step followed an E_1, E_2 or E_1cB pathway, depending upon the halogen in the quinone.

E_1

$$A + Y \underset{k_2}{\overset{k_1}{\rightleftharpoons}} \sigma \ (\text{Equilibrium}), \quad \sigma \xrightarrow{k_3} \sigma^+ + X^- \ (\text{Slow}), \quad \begin{cases} \sigma^+ + Y \xrightarrow{k_4} Z + YH^+ \\ \sigma^+ + B \xrightarrow{k_b} Z + BH^+ \end{cases} \ (\text{Fast})$$

E_1cB

$$A + Y \underset{k_2}{\overset{k_1}{\rightleftharpoons}} \sigma \ (\text{Equilibrium}), \quad \begin{cases} \sigma + Y \xrightarrow{k_3} \sigma^- + YH^+ \\ \sigma + B \xrightarrow{k_b} \sigma^- + BH^+ \end{cases} \ (\text{Slow}), \quad \sigma^- \xrightarrow{k_4} Z + X^- \ (\text{Fast})$$

A = monosubstituted product, Z = disubstituted product (**4** or **5**), σ = σ-complex, σ^+ = σ-complex after the loss of halide, σ^- is the σ-complex after the loss of a proton, B = organic base, X = Cl or Br.

Scheme 3

Thus for the disubstitution reaction we propose a mechanism involving an equilibrium between ylide **1** and the monosubstituted product **3** followed by elimination from the σ-complex either by an E_1 mechanism or an E_1cB route (Scheme 3).

If the steady state hypothesis may be applied to σ, σ^+ and σ^- intermediates and there is a large excess of ylide in the medium, the following equations [(19) and (20)] for the appearance of

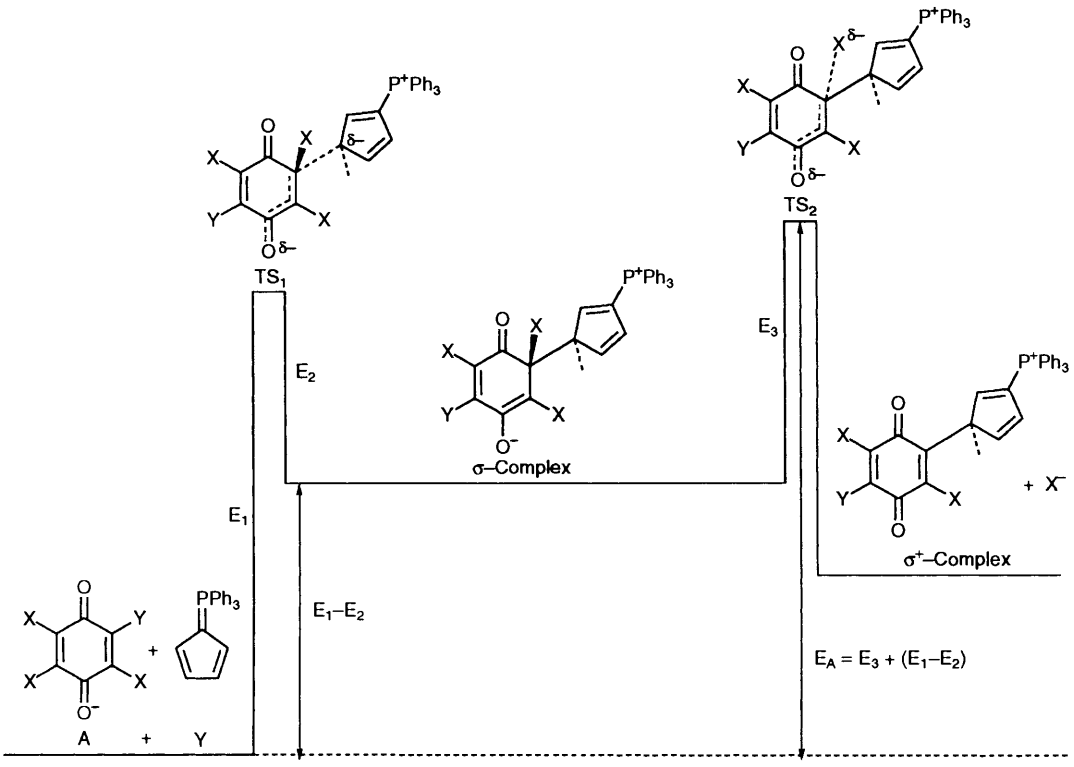

Fig. 10 Schematic energy diagram for the E_1 mechanism

Table 5 Thermodynamic activation parameters for the chloranil- and bromanil-ylide systems

	Chloranil		Bromanil	
Isomer	2,5-	2,6-	2,5-	2,6-
$\Delta H^{\ddagger}$/kJ mol^{-1}	39.0 ± 0.1	35.4 ± 0.1	41.7 ± 0.2	40.0 ± 0.4
$\Delta S^{\ddagger}$/J mol^{-1} K^{-1}	−129 ± 2	−142 ± 3	−116 ± 4	−121 ± 11
$\Delta G^{\ddagger}$/kJ mol^{-1}	76.8 ± 0.1	77.2 ± 0.1	75.7 ± 0.2	75.4 ± 0.4

each disubstituted compound are obtained, where $k_{obs} = k_g$ or

$$\dot{z} = \frac{k_1 k_3}{k_2 + k_3} y_o a = k_{obs} a \quad (E_1 \text{ mechanism}) \qquad (19)$$

$$\dot{z} = \frac{k_1 k_3 y_o^2 + k_1 k_b y_o b_o}{k_2 + k_3 y_o + k_b b_o} a = k_{obs} a \quad (E_1 cB \text{ mechanism}) \qquad (20)$$

k_v. The equations can be simplified in two extreme cases. For the E_1 mechanism depending on whether $k_2 \gg k_3$ or $k_2 \ll k_3$ equns. (21) and (22) are obtained:

$$\dot{z} = k_3 \frac{k_1}{k_2} y_o a = k_3 K_\sigma y_o a = k_{obs} a, \qquad K_\sigma = \frac{k_1}{k_2}$$
$$(k_2 \gg k_3) \qquad (21)$$

$$\dot{z} = k_1 y_o a = k_{obs} a \quad (k_2 \ll k_3) \qquad (22)$$

For the E_1cB mechanism, depending on whether $k_2 \gg k_3 y_o + k_b b_o$ or $k_2 \ll k_3 y_o + k_b b_o$ the equations for the limiting cases are (23) and (24).

$$\dot{z} = (k_3 K_\sigma y_o^2 + k_b K_\sigma y_o b_o) a = k_{obs} a \qquad (23)$$
$$(k_2 \gg k_3 y_o + k_b b_o)$$

$$\dot{z} = k_1 y_o a = k_{obs} a \quad (k_2 \ll k_3 y_o + k_b b_o) \qquad (24)$$

Only eqns. (19), (21), (22) and (24) give the observed dependence of k_{obs} on y_o and consequently the E_1cB cases with the condition applied in eqn. (23) can be rejected. Eqns. (22) and (24) are identical and can be derived supposing that the addition of the ylide to the quinone is the rate-limiting step of the reaction. If this assumption were true, however, the chloranil would react faster than bromanil since the withdrawing power of choranil and its derivatives is greater than that of bromanil. However, the experimental data suggest in fact, that the reaction for X = Br proceeds faster. On the other hand, the rate constant is unchanged by the presence of the amine (see Table 4) and no quadratic dependence of rate constant was observed in any of the cases studied. These facts suggest that the equilibrium hypothesis ($k_2 \gg k_3$) and the E_1 mechanism together explain the experimental observations better than the E_1cB mechanism. This conclusion is consistent with the fact that the dissociation energy of the C–Cl bond (338 kJ mol^{-1}) is higher than that of the C–Br bond (at 276 kJ mol^{-1}).

Interpretation of the Activation Parameters.—The activation parameters for the 2,6- and 2,5-disubstituted products of chloranil and bromanil are shown in Table 5. The experimental data indicate that in the case of chloranil, the 2,6-isomer forms slightly faster (k_g) than the 2,5-isomer (k_v). With bromanil the rates of formation of both isomers are essentially identical but slightly faster (1.4 and 1.9 times for 2,6- and 2,5-isomers, respectively) than for chloranil. The activation enthalpy and the entropy of activation are also identical within experimental error for the 2,6- and 2,5-isomers for bromanil with moderately

high negative entropies of activation (*ca.* -116 J mol^{-1} K^{-1}) compared with $\Delta S^{\ddagger} = -148$ J mol^{-1} K^{-1} for the reaction of ylide with bromanil to form the monosubstituted product. This suggests a lower degree of association in the transition state for disubstitution when compared with the transition state for the monosubstitution, a hypothesis which is substantiated by the activation enthalpy for disubstitution at 40 and 42 kJ mol^{-1} compared with *ca.* 12 kJ mol^{-1} for the monosubstitution reaction. This in turn, correlates with the suggestion that the formation of the σ-complex may be reversible with loss of the bromide ion as the rate-limiting step in the disubstitution process.

A similar picture emerges for chloranil for which the $\Delta S^{\ddagger}$ value for monosubstitution by the ylide is -140 J mol^{-1} K^{-1} (in dichloromethane) compared with -129 and -142 J mol^{-1} K^{-1} for 2,5- and 2,6-disubstitution, respectively. Again the slower rate for disubstitution *vs.* monosubstitution in the chloroquinone system is largely attributable to relatively high activation enthalpies of 39 and 35.4 kJ mol^{-1} for disubstitution compared with 13.6 kJ mol^{-1} for monosubstitution. However, the data are now indicative of an associative transition state for the 2,6-disubstitution which is similar to that for the ylide–chloranil monosubstitution reaction. With the relatively small differences in the activation parameters recorded for 2,5- and 2,6-substitution in chloranil it is difficult to draw definite conclusions but it seems that a decrease in activation enthalpy (for the 2,6-isomer) is compensated by a more negative entropy of activation relative to the 2,5-isomer.

The overall enthalpy change for the preferred E_1 mechanism to the 2,5-isomer (with $k_2 \gg k_3$) is shown in Fig. 10 in which the activation enthalpy of the reaction is represented by a combination of the addition and elimination steps.

Acknowledgements

We thank the *Fundación Ramón Areces* and DGICYT (PS90-0273) for support of this work and would like to acknowledge the contribution of the University of London Intercollegiate Research Service (Mrs. J. Hawkes and Mr. J. Cobb) in obtaining multinuclear NMR data.

References

1 F. Pérez Pla, J. Palou, R. Valero, C. D. Hall and P. Speers, *J. Chem. Soc., Perkin Trans. 2*, 1991, 1925.
2 R. Valero, F. Pérez Pla, J. Palou, C. D. Hall and P. Speers, *J. Chem. Soc., Perkin Trans. 2*, 1992, 425.
3 C. D. Hall, P. Speers, R. Valero, F. Pérez Pla and D. B. Denney, *Phosphorus, Sulfur, and Silicon*, 1989, **45**, 249.
4 C. D. Hall, P. Speers, R. Valero, F. Pérez Pla and D. B. Denney, *Phosphorus, Sulfur, and Silicon*, 1990, **49/50**, 143.
5 C. D. Hall, A. Sheridan, L. Shek, A. W. Parkins and S. C. Nyburg, *Phosphorus, Sulfur, and Silicon*, 1992, **69**, 167.
6 F. Ramirez and S. Levy, *J. Org. Chem.*, 1958, **23**, 2035.
7 C. D. Hall, A. W. Parkins and S. C. Nyburg, *Phosphorus, Sulfur, and Silicon*, 1991, **63**, 231.
8 T. Yamakoa and S. Nagakura, *Bull. Chem. Soc. Jpn.*, 1971, **44**, 2971.
9 A. Codoñer, I. Monzó, J. Palou and R. Valero, *J. Chem. Soc., Perkin Trans. 2*, 1988, 221.
10 I. Monzó, J. Palou, J. Roca and R. Valero, *J. Chem. Soc., Perkin Trans. 2*, 1988, 1995.
11 F. Ramirez and S. Levy, *J. Am. Chem. Soc.*, 1957, **79**, 67.
12 F. Pérez Pla, R. Valero, J. J. Baeza and G. Ramis Ramos, *QCPE Bulletin*, 1991, **11**, Program No. 605.
13 F. Pérez Pla, J. J. Baeza, G. Ramis Ramos and J. Palou, *J. Comput. Chem.*, 1991, **12**, 720.

Paper 4/01770F
Received 24*th March* 1994
Accepted 1*st June* 1994